RESEARCH ARTICLE

US East Coast offshore wind energy resources and their relationship to peak-time electricity demand

Michael J. Dvorak, Bethany A. Corcoran, John E. Ten Hoeve, Nicolas G. McIntyre and Mark Z. Jacobson

Atmosphere/Energy Program, Department of Civil and Environmental Engineering, Stanford University, 473 Via Ortega, MC 4020, Stanford, California, 94305, USA

ABSTRACT

This study characterized the annual mean US East Coast (USEC) offshore wind energy (OWE) resource on the basis of 5 years of high-resolution mesoscale model (Weather Research and Forecasting–Advanced Research Weather Research and Forecasting) results at 90 m height. Model output was evaluated against 23 buoys and nine offshore towers. Peak-time electrical demand was analyzed to determine if OWE resources were coincident with the increased grid load. The most suitable locations for large-scale development of OWE were prescribed, on the basis of the wind resource, bathymetry, hurricane risk and peak-time generation potential. The offshore region from Virginia to Maine was found to have the most exceptional overall resource with annual turbine capacity factors (CF) between 40% and 50%, shallow water and low hurricane risk. The best summer resource during peak time, in water of $\leq$50 m depth, is found between Long Island, New York and Cape Cod, Massachusetts, due in part to regional upwelling, which often strengthens the sea breeze. In the South US region, the waters off North Carolina have adequate wind resource and shallow bathymetry but high hurricane risk. Overall, the resource from Florida to Maine out to 200 m depth, with the use of turbine CF cutoffs of 45% and 40%, is 965–1372 TWh (110–157 GW average). About one-third of *US* or all of *Florida to Maine* electric demand can technically be provided with the use of USEC OWE. With the exception of summer, all peak-time demand for *Virginia to Maine* can be satisfied with OWE in the waters off those states. Copyright © 2012 John Wiley & Sons, Ltd.

1. INTRODUCTION

Offshore wind energy (OWE), located near large and dense coastal electricity demand centers, has the potential to provide large amounts of carbon-free power. Because OWE transmission cables are underwater, the burden of building new terrestrial transmission, which has been shown to be a limiting factor for land-based turbines,[1] is greatly reduced. In the USA, the majority of the population lives near oceans or the Great Lakes. As of 2003, 53% (153M people) lived in counties adjacent to oceans or the Great Lakes, with 23 of the 25 most densely populated US counties being coastal.[2] The 28 states that have coastal boundaries use 78% of the nation's electricity.[3] Of these 28 states, only six states have enough land-based wind resource potential to generate up to 20% of their electricity demand (see Department of Energy,[4] p. 48).

The 16 states and the District of Columbia from Florida to Maine near the coast (Figure 1) embody 34% of the total US electricity sales (2009),[5] 35% of the total US CO_2 emissions[3] and 37% of the US population.[6] The population density of the US East Coast (USEC) is both a benefit and a burden for the abatement of greenhouse gas (GHG) emissions. Dense populations allow a new electrical generation to serve a large number of people in a limited spatial area with limited investment in transmission. At the same time, states with high population densities and high demand for new transmission have the highest siting difficulties (specifically Maine, Massachusetts, Connecticut, New York and Pennsylvania; see
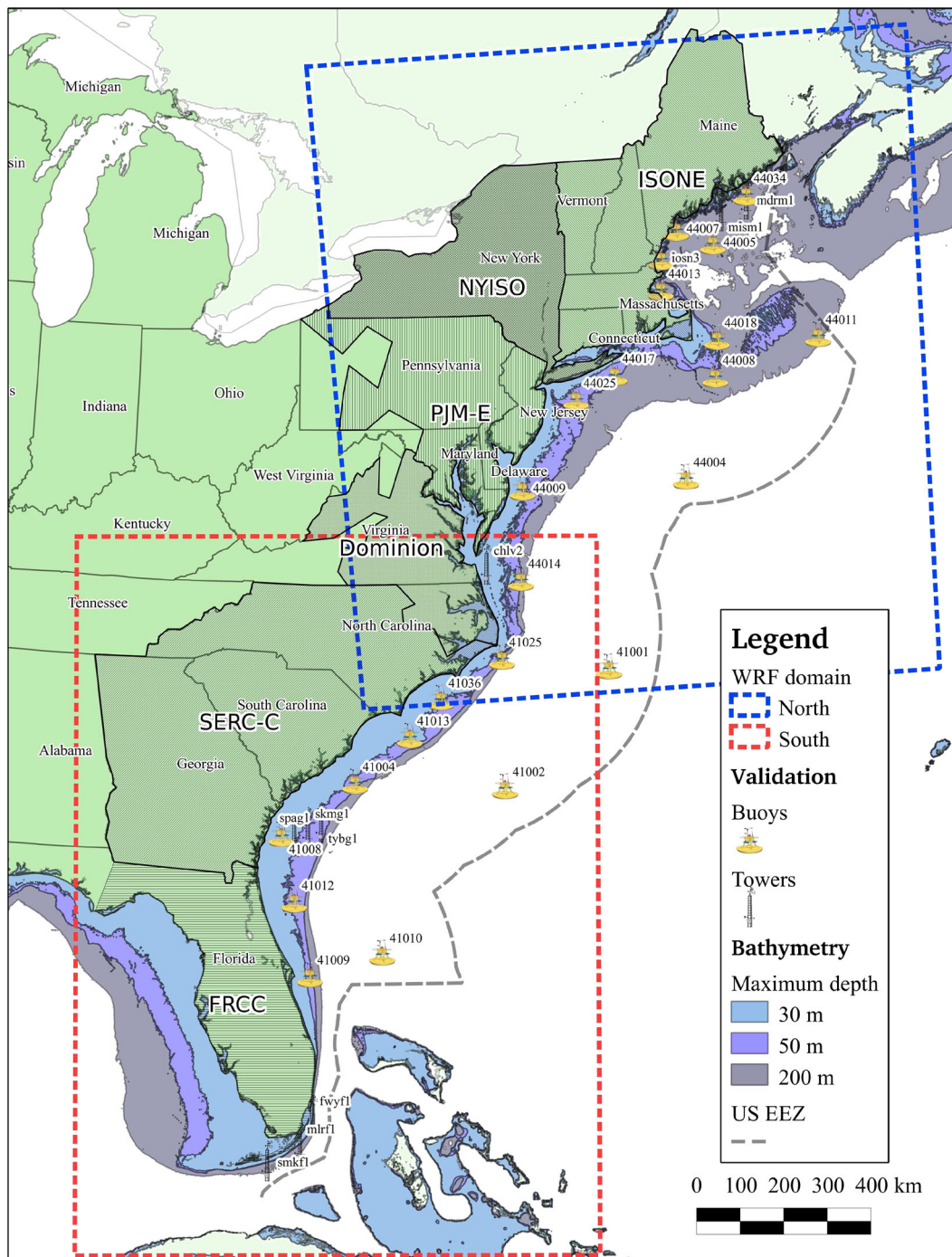
Figure 1. Overview map of the 5.0 km horizontal WRF-ARW modeling domains, validation buoys and towers, bathymetry classes, and demand regions. The study area was limited to waters within the US Exclusive Economic Zone (US EEZ) displayed on the map.

Vajjhala and Fischbeck,[7] pp. 660–661). Congestion has become an expensive problem in the Mid-Atlantic where transmission expansion has lagged demand. For example, congestion costs charged by the regional transmission operator (RTO) *PJM* were 3–9% of total energy market revenues between 2003 and 2010 (see PJM,[8] p. 472). OWE farms could ease transmission congestion in this region by putting large amounts of power generation online adjacent to the USEC.[9]

The USEC OWE resource has been roughly estimated to harbor hundreds of gigawatts of potential capacity,[10] although this resource has not yet been studied in significant temporal or climatological detail. Hart *et al.*[11] clarified the importance of obtaining more temporal and spatial detail in a wind energy resource analysis, particularly for determining the extent to which hourly demand for electricity can be met by renewable supply. It is known that aggregating wind power generation with transmission lines from multiple, geographically dispersed wind farms reduces the number of hours with no output and makes the total wind energy output probability density function more Gaussian than Weibull.[12] Kempton *et al.*[13] explored the utility of connecting offshore wind farms along the USEC by using buoy and reanalysis data, finding that wind farms connected ~1000 km apart and aligned with the prevailing frontal movements reduced ramp rates and lowered the number of no or full-power events. A high-voltage, direct current (HVDC) offshore transmission line called the *Atlantic Wind Connection* has been proposed from offshore New York to Virginia, and an alternative offshore grid location has been proposed, which takes advantage of sea breezes, spanning from Long Island, New York to the Georges Bank.[14]

In this study, we characterized the annual mean OWE resource and calculated the resource during periods of peak USEC electric demand on the basis of an analysis of electric demand data. The wind resource was modeled at potential locations with the use of a mesoscale weather model for 5 years at high resolution and validated with the use of a total of 32 buoys and offshore towers. This validation of a publicly available weather model provides insight into what the relative errors of forecasting USEC OWE might be if wind farms are built. The most suitable locations for large-scale development of OWE are prescribed on the basis of their wind resource, shallow bathymetry, hurricane risk and peak-power generation potential.

2. USEC WIND PATTERNS

The wind resource of the USEC is driven by a mix of synoptic-scale, mesoscale and climatological features. Sea and land breezes can vary on hourly timescales, large mid-latitude cyclones occur on the order of several days, and teleconnection patterns [e.g. El Niño and the North Atlantic Oscillation (NAO)] take place on the interannual timescale. This section gives an overview of the primary drivers of wind on the USEC, in order to guide the mesoscale modeling and analysis discussion.

2.1. Synoptic-scale meteorology

The region north of Virginia is dominated seasonally by nor'easters (northeasters) from November to April, whereas the Southeastern Coast has significant storm activity during June, September and October.[15] Developing mid-latitude cyclones traverse the continental USA and strengthen near the USEC.[16] As the surface front becomes occluded, these cyclones often begin to travel parallel to the coast rather than in the zonal direction, as the region of warm advection wraps poleward to the east of the cyclone's elevated trough and the region of cold advection heads equatorward to the west of the trough.[17] During the winter and spring in particular, strong temperature gradients resulting from relatively warm Gulf Stream-influenced tropical air masses to the east and cold continental polar air masses to the west can rapidly intensify a surface cyclone.[18] This extreme cyclogenesis, which often takes place along the Atlantic coast between New Jersey and Massachusetts, often results in nor'easters with strong winds.

There are two primary mechanisms for cyclogenesis along the USEC. Type I cyclones form along a surface front near the Gulf of Mexico and move northeastward along the Atlantic Coast.[16,19] Type II cyclones form as a secondary low to the southeast of a primary low located west of the Appalachians. This primary low is weakened by cold air damming east of the Appalachians, whereas coastal frontogenesis invigorates the secondary low off the mid-Atlantic coast.[20] The coastal front results from the strong temperature gradient between the cold dammed air to the west and the warm maritime air to the east. In these cases, a land breeze will often form and strengthen the synoptic-scale temperature and pressure gradients. Both type I and type II cyclones predominately move northward along the coast and reach a peak intensity somewhere off of New England or Nova Scotia before the surface front becomes fully occluded and temperature and upper-level vorticity advection cease.[16] A third system that can occasionally influence winds on the USEC during the winter is an Alberta Clipper. This fast-moving surface low from central Canada will occasionally cross the Appalachian Mountains, resulting in strong winds and cold temperatures.[21]

2.2. Mesoscale meteorology

During the summer months, the Northeast USEC often experiences its lowest wind speeds. Clear skies and slow winds are associated with a westward migration of the Bermuda-Azores High.[22] The mid-latitude storm track is located well to the north. Mesoscale wind systems such as sea and land breezes play a larger role during these months, particularly in the late spring and early summer when ocean temperatures are still relatively cold.[23] Six factors affect the formation and strength of these winds: (i) diurnal variation of the ground temperature, (ii) diffusion of heat, (iii) static stability, (iv) the Coriolis effect, (v) diffusion of momentum and (vi) prevailing wind, with the first three factors being the most important

(see Harris,[24] pp. 207–208). Additionally, upwelling off the New Jersey and New York coastlines provides an even greater land–sea temperature gradient and a stronger sea breeze.[25,26] The effect of the sea breeze can theoretically extend over a hundred kilometers offshore.[27] A modeling study by Colby[28] found a strong sea breeze off the southern coast of Connecticut, Rhode Island and Massachusetts during the summer months, likely due to the additive effect of the southerly sea breeze and the southerly winds of the westward side of the Bermuda-Azores High. Colle and Novak[29] (p. 2402) found that a low-level jet occurring in the New York Bight region could increase winds offshore when inland temperatures and electricity demand is high. Even though mesoscale winds dominate during these summer months, occasional moderate synoptic-scale westerly breezes can overcome the flow and kill the sea breeze.[30]

2.3. Climatology

It has been found that no significant long-term trend in USEC storm activity exists during the 20th century, although considerable interdecadal variability does exist.[15] One source of low-frequency variation is the NAO, which is a large driver of wintertime climate in the mid-to-higher latitudes of the North Atlantic. A standard deviation change of 1 in the NAO index leads to a small (≤ 0.5 m s^{-1}) change in the mean wind speed on the USEC (see Hurrell and Deser,[31] p. 34) and is therefore not a major driver of the total OWE resource adjacent to the USEC.

A second possible source of long-term variability is the El Niño/Southern Oscillation (ENSO). Alexander and Scott[32] (p. 46-2) found that the ENSO can warm the tropical North Atlantic and cool the Gulf of Mexico in the period following ENSO. In addition, the warm phase El Niño to cold phase La Niña anomaly on the USEC in winter (Dec, Jan, Feb) created more southward flowing surface winds on the order of 1 m s^{-1}, dropped surface pressure by 1–2 mb, and lowered sea surface temperatures (SSTs) by 0.3°C to 1.0°C. This El Niño minus La Niña anomaly represents the most extreme difference between climate modes, however. The actual differences between El Niño and normal or La Niña and normal would be less dramatic and have only minor influence on the USEC wind resource.

Climate change could also affect the wind resource off the USEC. Young *et al.*[33] found that the global ocean mean surface wind speed over the past 20 years has been increasing at a rate of 0.25–0.5% per annum.

3. PRIME LOCATIONS TO SITE WIND TURBINES

Our general goal was to find locations where offshore wind turbines could be placed with low hurricane risk and shallow bathymetry. We also generally calculated potential conflicts with preexisting and future offshore uses. The OWE resource potential was estimated with the use of a mesoscale weather model for the entire shallow water region of the USEC, both annually and during periods of peak coastal electricity demand. We assessed the climatological significance of the years chosen, based on historical records of coastal winds. These ideal attributes are combined to determine the most likely USEC offshore locations where future OWE development will occur in Section 5.

3.1. Low hurricane risk

Unlike their European counterparts, OWE farms on the USEC can be hit by powerful hurricanes, which frequent the USEC from June to November. Because hurricane intensity depends on warm water and moisture, hurricanes are less likely to remain strong over the cooler SSTs of the northeastern USEC (see McAdie *et al.*,[34] p. 28). Data from 1851 to 2006 show that the states of Maryland, Delaware, New Jersey, New Hampshire and Maine had no hurricanes greater than Saffir-Simpson (SS) category 2 (see McAdie *et al.*,[34] p. 33). The Mid-Atlantic and New England states that protrude from the coast (New York, Connecticut, Rhode Island and Massachusetts) experienced several hurricanes of SS category 3, but no SS category 4 or 5 hurricanes, during that same period (see McAdie *et al.*,[34] p. 33). The total number of SS category 3 hurricanes for these states from 1851 to 2006 are as follows: Virginia (one), New York (five), Connecticut (three), Rhode Island (four) and Massachusetts (three). No SS category 4 or 5 hurricanes have ever hit the region from Maine to Virginia from 1851 to 2006, and only 64 SS category 1–3 hurricanes have touched this same coastal area over the same period. In stark contrast are Southern states such as North Carolina and Florida. North Carolina experienced 47 hurricanes from 1851 to 2006, with 12 being SS category 3+. Florida had 144 hurricanes during this same period, with 37 being SS category 3+ (see McAdie *et al.*,[34] p. 33).

The practical implication of hurricane risk for OWE farms would be the inability of a developer to obtain insurance because the maximum design wind speed would be exceeded in a major hurricane. The International Electrotechnical Commission (IEC) and the Germanischer Lloyd classification society have formulated a set of design requirements for wind turbines to protect the turbine from damage throughout its working lifetime. With the absence of sea ice on the USEC, the two main sources of loading are wind and waves (see Twidell and Gaetano,[35] p. 233). Under the most strenuous

standard, IEC 61400-3 classified turbines are designed to withstand a maximum sustained wind speed of 50 m s^{-1}, corresponding to an SS category 3 hurricane (sustained winds of 50–58 m s^{-1}). This existing standard essentially precludes any location south of Virginia from turbine development.

3.2. Shallow bathymetry

In addition to an adequate offshore wind resource, the major limiting economic and technological factor for the development of offshore wind power is water depth. Similar to other studies (e.g. Dvorak *et al.*,[36] Dhanju *et al.*,[37] Lu *et al.*[38]), we chose bathymetry depth classes to approximately classify the current and future technological and economic constraints that may be encountered when developing the USEC OWE resource. It should be noted that the specific turbine foundation type used would be a project-specific engineering decision, taking into account the seabed (soil, slope and depth), and the force and fatigue loading from wind–sea interactions (wind, waves and currents). We generalized the turbine foundation classes on the basis of depth to illustrate the relative cost differences of developing wind farms in varying offshore regions.

A map of offshore depth contours (Figure 1) was created from a 30 arc sec global bathymetry data set.[39] We chose ≤30 m maximum depth for monopiles or gravity foundations (approximately consistent with existing projects),[40] 31–50 m for multi-leg foundations (see Twidell and Gaetano,[35] p. 206) and 51–200 m as the maximum depth that floating turbines could placed. Because floating turbines exist only as prototypes, this cutoff is hypothetical but consistent with a previous study performed for the California OWE resource.[36] Floating turbines will have a minimum depth of approximately 50 m and a maximum depth, past which the cost and required weight of moorings would be prohibitive (see Henderson AR, Witcher,[41] pp. 4, 13). For the USEC, the maximum depth is not so important in the New England and Mid-Atlantic region, as the continental shelf falls off rapidly after a 200 m depth, the depth which was used as the maximum for floating wind turbines. In the US Southern region, a large area would be available if waters ≥200 m are included, and floating turbines could be developed at greater depths.

3.3. Minimizing conflicting uses

Many competing commercial, recreational, military and environmental uses of the USEC offshore region exist. OWE farms would be sited with significant consideration of the impacts on these preexisting and competing uses. Dhanju *et al.*[37] analyzed the Delaware offshore region for uses that would potentially conflict with OWE projects. That study estimated the offshore areas that would be excluded by avian flyways, shipping lanes, chemical waste and explosives sites, military exclusions and beach nourishment borrow areas, in addition to a visual exclusion areas of 15 km offshore. The regions from 0–27 and 27–50 m depths were found to have 57% and 69% availability, respectively, with zero visual exclusion zone. When visual exclusion zones of 15 km were included, the available area was reduced to 34% and 69%, respectively. On the basis of this study, we assumed a one-third availability for the monopile depth class (1–30 m) and a two-thirds availability for both the multi-leg (31–50 m) and floating turbines (51–200 m) when calculating the overall OWE resource potential. Future studies should use modern marine spatial planning techniques to determine the precise amount of area that might be available for OWE.

4. OFFSHORE WIND ENERGY RESOURCE ESTIMATION

Several offshore wind field data exist for the USEC [e.g. QuikSCAT/SeaWinds, North American Regional Reanalysis (NARR) and Eastern Wind Integration and Transmission Study] but none with the spatial and temporal resolution that mesoscale modeling can provide. Our goal was to assess the accuracy of the mesoscale weather model Weather Research and Forecasting—Advanced Research WRF (WRF-ARW) to predict offshore wind fields and to present the validation results to the OWE community. Because one of the primary motivations of this research was to analyze the power generation potential of OWE during periods of peak demand, it is critical to have wind resource data at high temporal and spatial resolution for evaluation with available electric power demand data. Additionally, we wanted to resolve adequately the sea and land breeze in the near-coastal zone, which requires higher resolutions than the other wind field products provide.[28] As a result, we used WRF-ARW to model hourly winds at a high spatial resolution of 5 km for a period of 5 years and then validated the wind fields hourly by using a set of offshore buoys and towers.

4.1. Mesoscale wind modeling

A mesoscale weather model was employed to model turbine hub-height (90 m) winds of the USEC at high spatial (5×5 km) and temporal (1 h) resolution, the same resolution as in an OWE resource study off the coast of California.[36] The WRF-ARW mesoscale weather model[42] version 3.2.1 was run for five complete years of 2006–2010, and the winds were validated with 32 offshore buoys and offshore towers. WRF-ARW was run in parallel on the NASA Advanced

Supercomputing SGI-ICE Pleiades supercomputer and restarted every 4 days of model time to reset the initial conditions within the modeling domains. The internal time step was set by the adaptive time stepping scheme and had a mean of ∼21 s.

Several combinations of WRF-ARW domain configurations, planetary boundary layer (PBL) schemes, initial and boundary condition data sets, and SST data sets were tested for skill, with the current configuration having shown the most modeling skill[43] based on the criteria explained in Section 4.3. The entirety of the USEC was divided into two domains, *North* and *South*, shown in Figure 1. The North domain is a 267×293 point, 5.0 km resolution domain centered over the New England and the Mid-Atlantic border region. The South domain is a 240×330 point, 5.0 km resolution domain centered over South Carolina. The modeling domain extended sufficiently beyond the area of interest to limit the undesirable impacts of lateral boundary influenced winds, which is the reason for the overlap of the North and South domains shown in Figure 1. The vertical resolution of WRF-ARW contained 41 η_{half} levels, which included additional vertical levels at heights of interest for validation and wind resource assessment: 5 m for buoys, 45 m for offshore towers and 90 m for the assumed turbine hub height. Other WRF-ARW configuration options were as follows: Mellor–Yamada Nakanishi and Niino Level 2.5 PBL scheme, the Kain–Fritsch cumulus parameterization scheme and Monin–Obukhov surface layer physics. A constant sea surface roughness was found to be adequate for the purposes of wind resource assessment,[44] and we did not explicitly model wind stress and wave feedback in the surface layer.

The National Center for Environmental Prediction's NARR[45] was used to create initial and boundary conditions for the WRF-ARW runs. The NARR reanalysis data cover the entirety of North America, including the oceanic regions at 32 km horizontal, 45 layer vertical and 3-hourly temporal resolution. The NARR data set includes SST data from the 1° resolution Reynolds data set, which was updated every 4 days when WRF-ARW was restarted. Although it would be possible to analyze the OWE resource with the use of the lower-resolution reanalysis data alone, Colby[28] (p. 285) found that a 36 km spaced grid 'were able to develop a sea breeze circulation but without much detail'. Therefore, we have chose to use higher-resolution, 5 km spacing to better resolve the coastal region where sea breezes develop.

4.2. Climatological implications of modeled years

We modeled the winds for the five contemporary years, 2006–2010. This period was chosen because electric demand data along the entire USEC region were also available during the same period. We have also attempted to assess the climatological relevance of the years modeled.

To assess approximately the climatological validity of the years modeled, we used 6-hourly NCAR/NCEP Reanalysis Project $2.5 \times 2.5°$ data from 1949 to 2010 to analyze normalized wind speeds along the USEC region (see supporting information for more details). The NNRP 6-hourly data were standardized by the study years and compared with the mean wind speeds in the same region of the USEC from 2006 to 2010 in both the North and South domain regions (as defined in Figure 1). For the North domain, the standardized range for the five study years ranged from -1.6σ in 2009 to -0.4σ in 2007, indicating that the years studied were slower than average winds. The South domain was slightly closer to the mean, ranging from -1.4σ in 2009 to a nearly average of $+0.1\sigma$ in 2007. Assuming the reanalysis data are a proxy for the climatological mean, both of these findings suggest that the coastal OWE resource estimates we calculate here are conservative.

4.3. Validation of modeled winds

Hourly WRF-ARW output was validated with 23 buoys and nine offshore towers (see Figure 1 and the supporting information for the details of the locations). A criterion for evaluating modeled meteorological variables is set forth in Pielke[46] (p. 464) and was also used in a California OWE study.[36] In order to show modeling skill, a set of predicted wind speeds should have the following attributes: (i) $\sigma_{\text{WRF}} \approx \sigma_{\text{obs}}$, (ii) $RMSE < \sigma_{\text{obs}}$, and (iii) $RMSE_{\text{ub}} < \sigma_{\text{obs}}$, where σ_{WRF} is the standard deviation of the modeled field, σ_{obs} is the standard deviation of the observation, $RMSE$ is the root mean square error between the model and observations, and $RMSE_{\text{ub}}$ is the bias-corrected $RMSE$ (i.e. the bias is subtracted from v_{WRF} before calculating the $RMSE$).

The winds inside the coastal bays (e.g. Chesapeake, Delaware and Long Island Sound) were not validated. Therefore, the wind statistics in these bay regions should not be viewed as absolute. Because these winds are generally lower than their offshore counterparts and did not meet the minimum capacity factor (CF) threshold, as we set in Section 4.4, these bay areas were excluded from the overall OWE resource implicitly.

Aggregate annual validation statistics, grouped by year, are shown in Table I for buoy and offshore tower data. Because buoys and towers are often subject to harsh offshore conditions and hence failures, all statistics in the validation table are weighted by the count of available data points for that period. In the annual aggregate, all three validation criteria from Pielke[46] were met for both the North and South domains. Examples of the monthly time series of the u, v and wind speed magnitude, as well as the absolute error for u and v, are shown in Figure 2. As evidenced by example time series and

Table I. Summary validation results for each WRF-ARW modeled year.

	Buoy		WRF		Validation stats				
	Mean m/s	σ m/s	Mean m/s	σ m/s	*RMSE* m/s	$RMSE/\sigma_{buoy}$	$RMSE_{unbiased}$ m/s	Bias m/s	Count
(a) Buoy validation									
North domain									
2006	6.54	3.00	6.65	2.97	2.07	0.69	1.98	0.11	92,603
2007	6.80	3.02	6.83	2.96	2.06	0.68	1.95	0.03	113,573
2008	6.71	3.06	6.63	2.94	2.12	0.70	2.01	−0.08	98,897
2009	6.78	3.01	6.70	2.88	2.18	0.72	2.03	−0.08	82,277
2010	6.83	2.98	6.79	2.92	2.14	0.72	2.03	−0.04	78,865
South domain									
2006	6.36	2.81	6.50	2.79	2.23	0.79	2.17	0.14	75,553
2007	6.60	2.95	6.60	2.84	2.18	0.74	2.12	0.01	73,638
2008	6.69	2.98	6.80	2.98	2.22	0.75	2.17	0.11	74,007
2009	6.38	2.73	6.55	2.82	2.36	0.86	2.28	0.17	61,298
2010	6.45	2.71	6.77	2.76	2.16	0.80	2.08	0.32	57,439
(b) Offshore tower validation									
North domain									
2006	7.75	3.45	7.62	3.55	2.48	0.70	2.42	−0.13	24,827
2007	8.10	3.73	8.14	3.80	2.47	0.65	2.41	0.04	23,571
2008	8.10	3.69	8.03	3.73	2.50	0.67	2.43	−0.07	23,916
2009	8.34	3.73	8.14	3.68	2.62	0.71	2.52	−0.21	13,315
2010	8.52	3.71	8.30	3.80	2.43	0.64	2.36	−0.21	11,739
South domain									
2006	6.99	3.06	6.46	2.96	2.56	0.86	2.45	−0.53	47,226
2007	7.08	3.23	6.42	3.07	2.60	0.85	2.45	−0.66	41,300
2008	7.28	3.12	6.49	2.98	2.46	0.82	2.27	−0.79	34,762
2009	6.74	2.86	6.37	2.85	2.52	0.88	2.41	−0.37	32,567
2010	7.11	3.04	6.66	2.96	2.41	0.81	2.32	−0.45	29,912

aggregate validation statistics, WRF-ARW was generally skilled at predicting both the magnitude and direction of the winds at the validation locations. Several short spikes of absolute error can be noticed in the bottom of the plots, which is likely due to WRF-ARW incorrectly predicting the time of a passing front by 1 or 2 h (e.g. the bottom pane of absolute error in Figure 2(b and f)); this is not an uncommon problem when using a mesoscale model for this purpose (see Colle and Novak,[29] pp. 2402–2403). For the purposes of OWE resource assessment, it is more important to match the overall variability of the resource ($\sigma_{WRF} \approx \sigma_{obs}$) rather than the exact timing of passing fronts over the long-term analysis period.

WRF-ARW modeled the winds at the 23 buoys with skill in the annual aggregate for all five model years in both domains (see Table I(a) and Figure 1 for locations of the buoys and towers). The modeled variability of the winds (σ_{buoy}) matched the data well, with 4.6% error in the North domain for 2010 being the largest discrepancy between σ_{buoy} and σ_{WRF} in the annual aggregate, although some buoys had slightly higher individual discrepancies, as shown in Figure 2(a–c). All RMSE values were well below criterion (ii) (see Table I(a) column $RMSE/\sigma_{obs}$, which should be <1). The bias for the buoy winds was low, and criterion (iii) was satisfied.

WRF-ARW also showed similar modeling skill at each of the nine offshore tower validation locations. The WRF-ARW 45 m height was used to compare with all offshore tower heights, which ranged from 16 to 50 m in height. A comparison of WRF-ARW winds at higher or lower height winds adds some bias to the validation, evidenced by the slightly higher bias values in Table I(b) than the buoy validation biases in Table I(a). The vertical scaling of wind speed from 16 to 45 m is only 8% different assuming a log-law vertical profile and a neutrally buoyant boundary layer and 5% different from 16 m, the lowest tower height to 45 m (see supporting information for details).

4.4. Annual resource calculation method

In order to calculate the gross OWE resource, we made certain simplifying assumptions about usable waters for wind farms and the wake losses associated with wind turbine arrays. Such assumptions are common for estimating global wind power potential (e.g. Lu *et al.*,[38] Archer and Jacobson,[47] Liu *et al.*,[48] Capps and Zender[49]), as well as regional wind resource
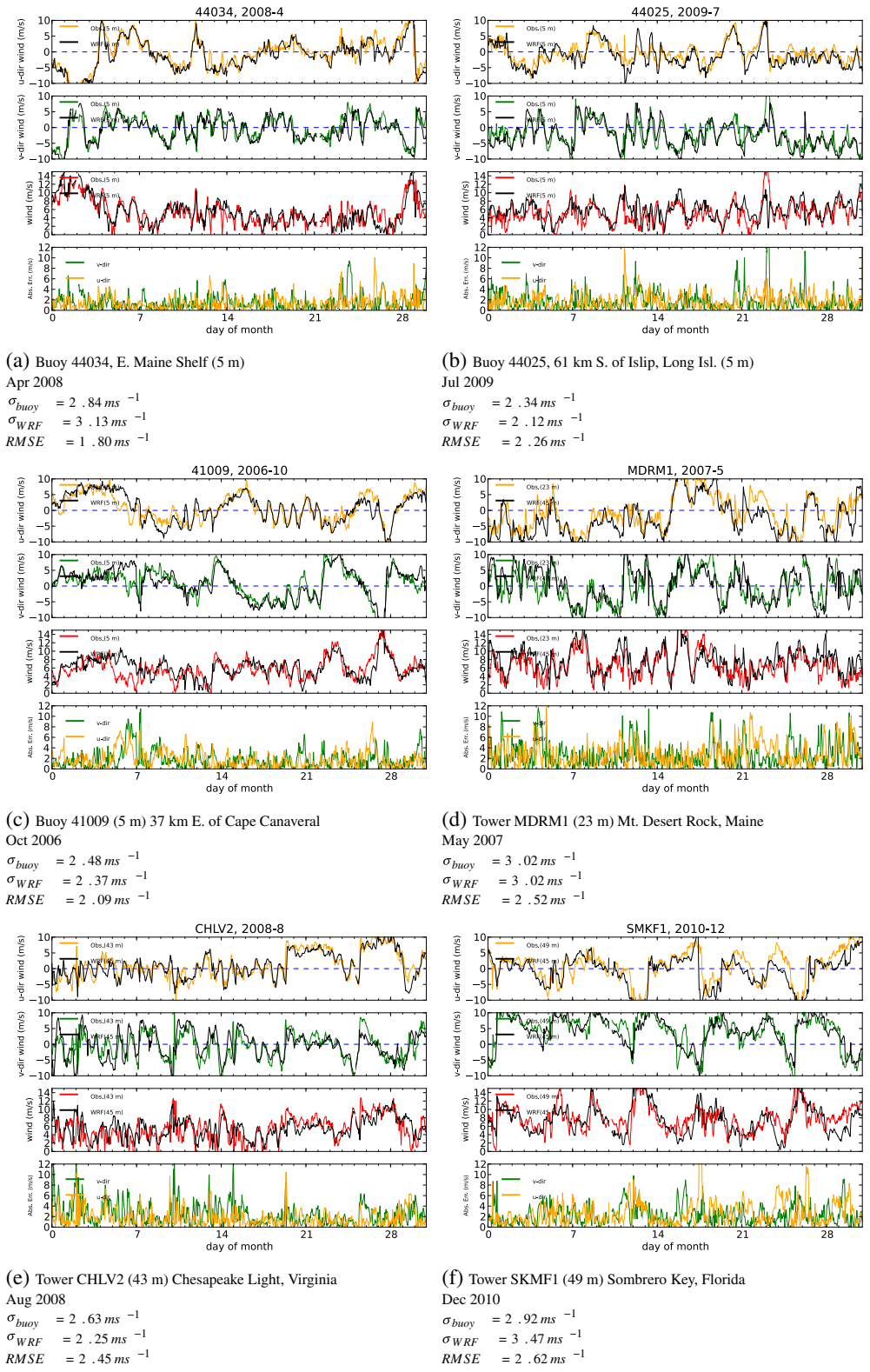
Figure 2. Six months' worth of example validation time series for three buoys (a–c) and three offshore towers (d–f), along with the validation statistics, with black lines representing WRF-ARW predictions and colored lines observations. From top to bottom: *u*-wind, *v*-wind, wind speed and abs. error for *u* (yellow) and *v* (green) directions.

assessments.[36,37,50,51] In addition to estimating the conventional resource statistics of mean wind speed and mean power density, we have estimated the CF by using a representative wind turbine power curve. We integrated the power curve from a REpower 5M 5.0 MW turbine at the 90 m height for all hours of the year (see supporting information Section S4 for details).[*] An added benefit of using a turbine power curve is that it includes mechanical and electrical losses, so no further assumptions are needed to be made about the power delivered from the turbine (see supporting information for the power curve).

We assumed 10% wake losses in energy, on the basis of wake loss modeling and measurements at a Danish offshore wind farm that had close turbine spacing of 2.4 diameters (D).[52] We chose a more conservative turbine spacing of 10 diameters square ($10D \times 10D$), which equates to 3.15 MW km^{-2} density, using the REpower 5M 5 MW rotor diameter of 126 m. Projects could be built with the use of a more compact (e.g. $10D \times 3D$) spacing, potentially to reduce undersea cabling costs or to take advantage of a consistent wind direction, but array losses would be higher for some wind directions. Therefore, we stick with the more conservative $10D \times 10D$ spacing. Wind farm availability was estimated to be 91% in a modeling study.[53] Another study analyzed trends in availability and estimated future availability to be 97% (see Levitt,[54] p. 6412). Because of differences in these studies, we used the mean of these two studies, 94% for our wind farm availability factor. Transmission line losses are small, with 3% being a good estimate for an appropriately designed HVAC or HVDC system up to 100 km in length.[55] When combined multiplicatively, the assumed wind farm availability, wake and transmission energy losses total 17.9% at each potential wind farm location.

Compared with wake and transmission assumptions, the most variable factor is the conflicting use assumptions outlined in Section 3.3, with one-third of the energy in water with depth $\leq$30 m and two-thirds of the energy for waters >30 m and $\leq$200 m being developable. We disaggregated the resource by the water depth classes defined in Section 3.2. All of these assumptions, including the observation that the years modeled had on average slightly lower annual wind speeds (see Section 2.3), combine to make this a conservative calculation of the USEC wind resource.

5. RESULTS AND DISCUSSION

The annual OWE resource was mapped for the entire USEC from Florida to Maine based on the mean wind speed, mean power density and CF for a representative 5.0 MW offshore turbine, with the use of the hub height that OWE wind fields developed in Section 4. CF is the actual amount of energy generated by a turbine over the course of a year compared with the amount of energy that would be generated if the turbine ran at nameplate capacity all year. We use two CF figures uniformly in the following sections. CF_{gross} is the raw energy at the turbine without any losses. CF_{net} takes into account wake losses, transmission losses and mechanical availability. Using only the best OWE resources based on CF_{gross}, we determined the total amount of electricity that could be generated from USEC OWE and compared that with US and USEC electricity demand. We combined the 'prime locations' for USEC OWE (Section 3) results, a peak-time electricity demand analysis based on 4–5 years of hourly coastal electric demand, and annual resource assessment maps to determine locations that are best suited to generate electricity when electric demand is highest. The OWE resource in this subregion from Virginia to Maine is analyzed in detail, with the resource characterized by turbine foundation depth class, seasonal generation during peak time and the interannual variability by season. Lastly, we compared and contrasted these new OWE resource maps with existing maps of the same area.

5.1. Annual offshore wind energy resource and bathymetry

The overall annual OWE resource, based on the five study years of 2006–2010, is mapped in terms of mean wind speed, mean wind power density and CF_{gross} in Figure 3(a–c), respectively. Locations with annual mean $CF_{\text{gross}} \geq 45\%$ and $CF_{\text{gross}} \geq 40\%$, based on the five study years, are listed in Table II, divided into the turbine foundation depth classes defined in Section 3.2. The total number of turbines per area was calculated as described in Section 4.4. The wind resource is highest in New England with a mean wind power density of nearly 1000 W m^{-2} ($CF_{\text{gross}} \approx 51\%$) on the Georges Banks, east of Massachusetts. The wind resource gradually diminishes southward towards the Gulf of Mexico, where the power density is only 250 W m^{-2} ($CF_{\text{gross}} \approx 21\%$).

The locations likely to be economically viable at current wind turbine installation costs all lie within the North domain (Figure 1), which is coastal North Carolina and the offshore areas northward (mean power density $\geq$600 W m^{-2} in Figure 3(b) and $CF_{\text{gross}} \geq 40\%$ in (c)). Most of the resource lies in deep water (Table II, 51–200 m depth) and would require the development of floating turbines and an offshore grid to fully exploit the resource.

Shallow water regions, unlike the wind resource, which has disproportionately stronger winds in the North domain, are spread more evenly between the North and South domains (Figure 1). The amount of offshore surface area in the monopile (1–30 m), multi-leg (31–50 m) and floating (51–200 m) depth classes contained within boundaries of the North and South

---

[*]Supporting information may be found in the online version of this article.

(a) Mean wind speed (ms^{-1})   (b) Wind power density (Wm^{-2})   (c) REpower 5M, 5MW turbine capacity factor)
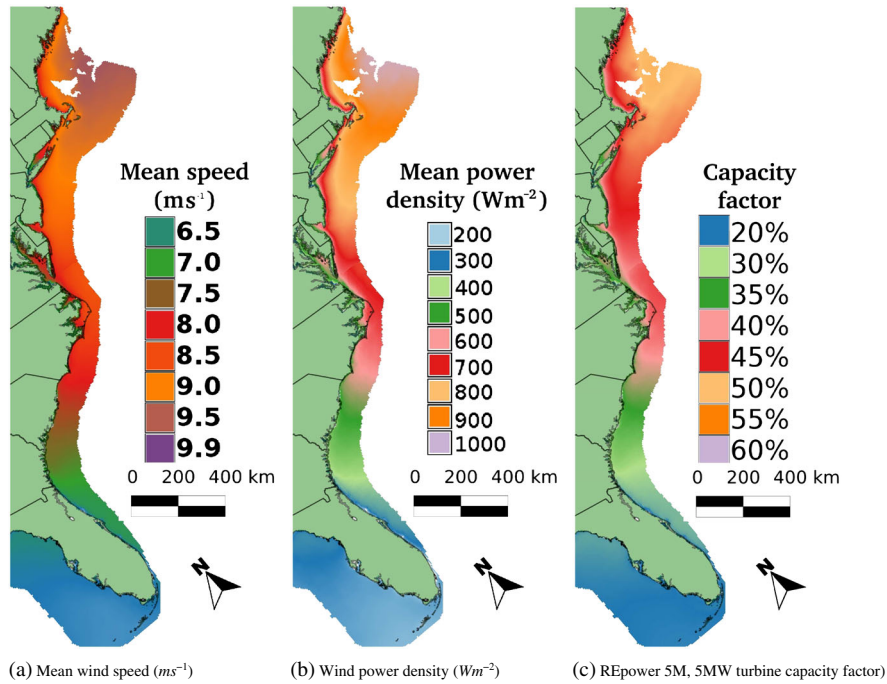
Figure 3. Annual, 24-hourly wind resource of the US EC at the 90 m hub height for the modeled years 2006–2010.

Table II. Annual mean OWE energy statistics for combined North and South domain areas for 5.0 MW turbine, based on the five modeled years of 2006–2010.

Depth (m)	Area (km^2)	5 MW turbines	Availability	Capacity (GW)	Mean CF (%)	Mean power (GW)	Annual energy (TWh)
(a) $CF_{gross} \geq 45\%$							
1–30	10,125	2k	1/3	11	48.2	4.2	37
31–50	25,750	11k	2/3	54	47.9	21.3	186
51–200	101,550	43k	2/3	213	48.4	84.6	741
1–200	137,425	56k		278	48.3	110.4	965
(b) $CF_{gross} \geq 40\%$							
1–30	47,875	10k	1/3	50	43.4	17.9	157
31–50	49,825	21k	2/3	105	45.5	39.0	342
51–200	121,775	51k	2/3	256	47.5	99.7	873
1–200	219,475	82k		411	46.5	156.6	1372

The total CF_{gross} is a weighted mean, weighed by *capacity*. The loss factor of 17.9% stated in Section 4.4 was applied to the mean power and annual energy calculations.

WRF-ARW modeling domains shown in Figure 1 is 506k, 200k and 455k km^2, respectively. Relative to the land surface area of the New York state, these offshore areas are about 3.6, 1.4 and 3.2 times larger, respectively, which has a land and territorial water area of 141,299 km^2 (see USCB,[56] p. 71).

The entire wind resource in bulk, with the use of only high-quality OWE areas with $CF_{gross} \geq 45\%$ and $CF_{gross} \geq 40\%$, could provide up to 965 and 1372 TWh of energy annually (110–157 GW average), respectively. If the turbine spacing was reduced from $10D \times 10D$ to a more compact $10D \times 3D$, this amount could grow by possibly a factor of 3, although array losses would be higher. To put this amount in perspective, the amount of electricity sold in the entire US was 3597 TWh for 2009,[3] which the USEC wind resource alone could provide 24–35% of. The resource could provide 79–112% of the electricity for the USEC states (1227 TWh in 2009) from Florida to Maine. A likely near-term scenario is only developing the shallow water area regions out to 50 m depth, which excludes floating turbine technology. With the use of the 45% and 40% CF_{gross} cutoffs, these shallower waters could provide between 6–13% of US and 18–41% of USEC 2009 electricity sales.

5.2. Characterization of regional electric demand

Our principal objective was to analyze the USEC OWE resource during times of peak electricity demand seasonally and by depth, as well as the interannual variability of the peak-time resource. OWE that could be supplied during hours of peak demand is more valuable for reducing GHG emissions and consumer cost than energy supplied during off-peak hours. We examined all reporting coastal load serving entities of the USEC to determine the time and magnitude of peak electricity demand. Independent system operators (ISO) and RTOs control the electric power system through coordination of generation and transmission resources. The balancing areas and utilities included in this study have varying definitions of peak-rate hours, based on their respective demand profiles. Since we are not specifically interested in the *exact* impact of OWE on electricity rates, we designed a uniform and rate-independent method to determine an overall yearly peak-demand period for all USEC regions. We defined the hours of peak demand as the *first* and *last* hours the daily demand went *above* and *below* the median value, respectively (see supporting information Section S3.1 for details).

5.2.1. Determining the annual-peak demand period.

Hourly demand data from ISO New England (ISO-NE), New York ISO (NYISO) and PJM Interconnection (PJM) were analyzed for 2006–2010. The *coastal* region of the Southeast Electric Reliability Council (SERC), which we called SERC-C, and the Florida Reliability Coordinating Council (FRCC) data were analyzed from 2006 to 2009. The extent of each region is mapped in Figure 1. The power system demand was calculated seasonally with the use of hourly data available from all aforementioned entities. Daylight saving time (DST) was removed from the demand data by converting to Eastern Standard Time (EST) (Coordinated Universal Time − 5 h). Details of the analysis can be found in the supporting information (Section S3.2).

The peak duration column in Table III shows the mean start and end hours of the peak-time period by season and USEC region. The times and duration of the peak-time period vary by season, with summer having the shortest period and winter having the longest. We average all seasons to obtain a single peak-time period. The mean of the start and end hours of the peak-time for all seasons are 08:08 and 20:53 EST, respectively. The weighted mean, weighted by 'peak annual energy use' in each region, is nearly the same with 08:03 and 20:54 EST, respectively. On the basis of these results and rounding to the nearest hour, we concluded that the overall peak-time period, based on our median threshold criteria for the entire USEC region, starts at 08:00 and ends at 21:00 EST. Although this is a generalization, this is somewhat consistent with utility definitions for peak-time on the USEC (see supporting information for discussion). These peak times could change in the future if there was large-scale implementation of new technologies such as electric vehicle charging or demand response. Because of the flexibility in controlling these new technologies, peak-demand could become longer but lower in magnitude.

5.2.2. Seasonal and regional demand.

Results of the electric demand analysis for peak magnitude and time, peak duration and average annual energy use are given in Table III by season and USEC region. The electric demand data analyzed for this study had distinctly different seasonal and regional demand profiles, primarily because of varying heating and cooling needs.

The winter season electric demand profile was generally characterized by a double peak in mid-morning and early evening. This winter double peak was more prevalent in the southeastern regions (PJM-DOM, SERC-C and FRCC), where heating needs are met primarily with electric heaters,[57,58] and less pronounced in the remaining USEC regions (ISO-NE, NYISO and PJM-E), where natural gas and fuel oil satisfy most heating requirements.[59–61] The results in Table III support these regional and wintertime traits, as the winter season consistently had the longest peak-demand duration, especially for the PJM-DOM and SERC-C regions.

The summer season demand profile had a single, large peak in mid-afternoon due largely to air conditioning (AC) demand, which is more significant in the hotter southeastern regions.[57] This is consistent with the results in Table III, as the summer peak-demand duration was on average shorter than the winter peak duration by 2 h and 40 min for all regions. In addition, the mean-peak magnitude was on average for all regions the smallest in the winter and largest in the summer, likely driven by the more sizable summer AC demand.

Two of the southeastern regions, SERC-C and FRCC, exhibited the most extreme characteristics of all USEC regions. The SERC-C coastal region consistently had the largest mean-peak and maximum peak magnitudes, likely due to the elevated electric heating demand in winter and even greater AC demand in summer. The FRCC region consistently had the largest ratio of maximum to minimum demand, indicating that the FRCC region had the greatest variation in daily demand of all USEC regions. The FRCC region average ratio of maximum demand to minimum demand over all seasons was 1.81, which represents an 18% greater variability in demand than the average ratio over all seasons for the remaining USEC regions of 1.53. This variation was the smallest in the winter and largest in the summer, most likely due to the mid-morning and early-evening winter electric heater usage and large mid-afternoon summer AC demand.

Table III. Peak-time electricity demand characteristics grouped by region and seasonal months using 2006–2010 data for all regions except for SERC-C and FRCC, which used 2006–2009 data.

Months	Region	Subregion	Peak magnitude and time Mean time (EST)	Mean (GW)	Max (GW)	Max:min	Peak duration Mean start (EST)	Mean end (EST)	Peak annual energy use Mean (GWh)
Winter Jan, Feb, Mar	ISONE		17:16	15.8	35.7	1.53	07:19	20:45	44,354
	NYISO		17:37	21.4	25.1	1.45	08:21	20:56	25,333
	PJM	PJM-E	16:21	37.8	48.5	1.36	06:50	21:25	47,735
		DOM	11:52	12.9	18.1	1.38	05:30	21:34	17,676
	SERC-C		11:41	44.6	65.3	1.39	05:24	21:30	64,223
	FRCC		15:51	28.0	46.1	1.70	07:56	21:08	31,751
Spring Apr, May, Jun	ISONE		14:27	32.4	51.4	1.59	07:33	19:47	36,888
	NYISO		14:42	20.5	32.4	1.51	08:00	19:59	23,427
	PJM	PJM-E	16:29	36.1	59.7	1.52	08:54	21:13	40,655
		DOM	16:32	12.2	19.1	1.61	09:05	21:26	13,529
	SERC-C		15:42	46.4	67.9	1.62	08:44	21:06	51,103
	FRCC		15:29	34.6	46.2	1.92	09:31	21:29	35,049
Summer Jul, Aug, Sep	ISONE		14:28	37.7	55.2	1.66	08:15	19:42	43,093
	NYISO		14:40	24.2	33.9	1.54	08:29	19:57	27,617
	PJM	PJM-E	16:03	43.3	62.0	1.62	09:45	21:14	45,406
		DOM	16:11	14.8	19.7	1.72	09:51	21:25	15,327
	SERC-C		15:15	55.3	71.9	1.72	09:10	21:07	61,058
	FRCC		14:50	39.3	46.2	1.87	09:22	21:18	43,000
Fall Oct, Nov, Dec	ISONE		16:48	34.6	41.8	1.63	07:51	20:28	37,916
	NYISO		17:07	20.9	25.8	1.53	08:21	20:56	23,285
	PJM	PJM-E	17:39	35.9	47.6	1.45	07:48	21:21	43,050
		DOM	14:50	11.8	17.7	1.45	06:43	21:29	14,944
	SERC-C		14:20	41.9	58.1	1.41	06:33	21:25	52,745
	FRCC		16:33	29.7	42.2	1.75	08:53	21:17	32,495

Start times are in Eastern Standard Time and *do not* include a daylight saving time shift. *Peak start* and *end* are defined as the mean time the demand first *goes above* and last time it goes *goes below* the median demand value for that day, respectively.

5.3. Prime locations for peak-power generation: New England and Mid-Atlantic

The continental shelf of the USEC extends out especially far in the regions off Massachusetts, New Jersey, Delaware and Virginia, with depths of ≤ 50 m being found as far out as 80 km. This shallow water, combined with an exceptional OWE resource, a large coastal population, an aging and congested land-based grid, low severe-hurricane risk and relatively high electricity prices, makes this an ideal location for large OWE farms. We used the peak-time electric demand results from Sections 5.2.1 and 5.2.2 to determine the peak time, seasonal wind resource and interannual variability of the peak in this region.

As an *a priori* requirement, we limited OWE development to locations where the mean 5 year OWE resource has $CF_{gross} \geq 45\%$ annually, from the south border of Virginia to Maine (VA-to-ME). These regions can be identified in Figure 3(c) where $CF_{gross} \geq 45\%$ for regions north of the Virginia southern latitude at the coast ($36°33'$N). Peak-time seasonal demand of the ISONE, NYISO, PJM-E and DOM regions (Section 5.2) was compared with the peak resource based on the REpower 5M 5.0 MW turbine power curve (see supporting information) integrated hourly. The OWE resource was grouped by seasons and turbine foundation depth classes. Ranges of uncertainty for the peak resource were presented as the minimum and maximum resources of each WRF-ARW 5.0×5.0 km^2 grid cell over the five study years. All of the assumptions of wake and transmission losses and offshore availability (Section 4.4) were applied in the same manner as the resource calculations in Section 5.1 and Table II.

The calculation generalizing seasonal electricity demand and wind resource did not take into account the diurnal variability present in demand and the wind resource. Rather, we dealt with peak-time variability in the aggregate by depth classes and seasons. Our primary goal was to determine how much peak resource could be delivered at each depth class, during each season. This also gives insight into the amount of each turbine foundation technology required to satisfy peak demand. Results are summarized in Table IV and further analyzed in the next three sections by season and depth.

5.3.1. Winter and fall peak-time resource.

The winter and fall seasons are dominated by large, mid-latitude cyclones that move northward up the coast, reaching their maximum strength in New England (see Section 2.1 for a discussion). These large and powerful storms could cause wind farms to run at their rated power for several days on end. The wintertime mean-peak wind resource (Figure 4(a)) from 08:00 to 21:00 EST is very high, with $CF_{gross} \geq 50\%$ for most regions. If the peak-demand period was to change, because of large-scale implementation of load shifting technologies (e.g. electric vehicles or demand response), the storm-driven OWE resource would not change substantially because storms are not tied to a diurnal cycle. Some far offshore regions off New Jersey and northward have CFs as high as 65%. Near Cape Cod, Massachusetts, CF_{gross} is as high as 60% exist only a few kilometers offshore.

This powerful wintertime peak resource is well suited for the USEC wintertime peak demand; all electric demand regions with the exception of the FRCC and NYISO in Table III have a maximum seasonal mean-peak annual energy use in the wintertime. Arctic fronts and Alberta Clippers bring bitterly cold Canadian air to the USEC, resulting in increased heating demands throughout the VA-to-ME region. The winds associated with these fronts could power the elevated electric heating loads in the southern sections of the VA-to-ME region[57] and help alleviate the natural gas shortage for electricity generation caused by natural gas supplies being diverted to space heating (see CapeWind Associates LLC,[62] p. 7).

The fall resource shown in Figure 4(d) is similar to the wintertime resource, with most of the Mid-Atlantic and New England having an extremely strong peak-time resource with $CF_{gross} \geq 45\%$. The CF_{gross} from eastern Long Island to the Cape Cod region is especially similar to the winter resource. CFs are as much as 5% lower off New Jersey, Delaware, Maryland and Virginia compared with those of the Cape Cod region.

The strongest peak resource off the USEC can be found in the shallow waters of the Georges Banks off Cape Cod, Massachusetts. This impressive resource boasts $CF_{gross} \approx 60\%$ during the wintertime and $CF_{gross} \approx 55\%$ in the fall. This historic fishing ground has waters as shallow as only a few meters deep, despite being 150 km from Cape Cod. Development in this potentially sensitive ecosystem would have to proceed carefully.

5.3.2. Spring and summer peak-time resource.

The springtime mean-peak wind resource shown in Figure 4(b) from 08:00 to 21:00 EST is diminished from the winter and fall months but is still strong, with CF_{gross} in the 40–50% range. The winds are noticeably strong northeast of Block Canyon, off the southeastern tip of Long Island. This is consistent with other studies that have found enhanced upwelling in this region due to the a predominately southwestely wind driven by the Bermuda-Azores High.[25,26] Mean SST temperatures in this region during the spring months from 1985 to 2001 range from 14°C off southeastern Long Island to 9°C near Nantucket Island—a pronounced difference of 5°C[63] (see supporting information Figure S5).

During the summertime, the mean-peak wind resource from 08:00 to 21:00 EST (Figure 4(c)) is markedly diminished from Virginia up to the New York Harbor, with CF_{gross} around 30–35%. From Long Island to Nantucket Sound, peak time CF_{gross} remains strong with $CF_{gross} \geq 40\%$. This dramatic difference is likely caused by the difference in SSTs between

Table IV. Seasonal, peak (08:00–21:00 EST) energy use in the ISONE, NYISO, PJM-E and DOM regions that could be satisfied with OWE based on the peak annual energy use results in Table III and using only sites with $CF_{gross} \geq 45\%$ in the 5 year, 24-hourly mean at the 90 m height.

Depth range (m)	Winter			Spring			Summer			Fall		
	Mean (%)	Δmin (%)	Δmax (%)	Mean (%)	Δmin (%)	Δmax (%)	Mean (%)	Δmin (%)	Δmax (%)	Mean (%)	Δmin (%)	Δmax (%)
1–30	4.2	−0.3	0.5	4.3	−0.4	0.6	2.9	−0.2	0.2	4.4	−0.4	0.4
31–50	21.7	−1.5	2.4	22.1	−1.7	2.9	14.4	−1.3	1.4	23.0	−1.9	2.5
51–200	86.5	−6.0	9.3	86.6	−7.0	11.2	57.0	−4.8	6.2	90.9	−7.6	10.2
Total	112.3	−7.9	12.2	113.0	−9.1	14.7	74.3	−6.3	7.9	118.4	−9.9	13.1

Variability percents were calculated with the use of the 5 year minimum and maximum OWE resources for each WRF-ARW 5.0 × 5.0 km² grid cell (Δ min and Δ max). The loss factor of 17.9% stated in Section 4.4 was applied to these calculations.
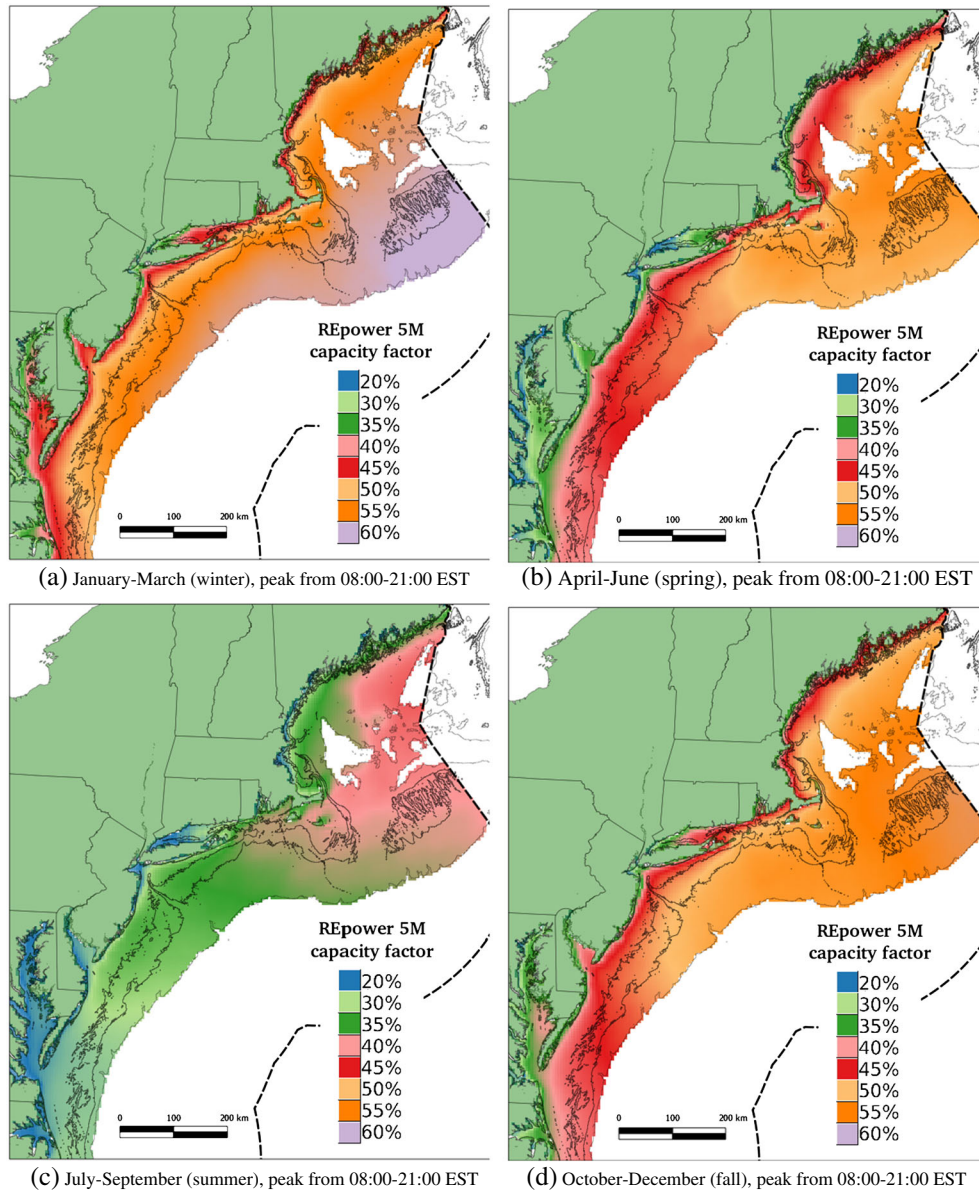
(a) January-March (winter), peak from 08:00-21:00 EST

(b) April-June (spring), peak from 08:00-21:00 EST

(c) July-September (summer), peak from 08:00-21:00 EST

(d) October-December (fall), peak from 08:00-21:00 EST

Figure 4. Ninety meter seasonal *peak-time* (08:00–21:00 EST) wind resource maps of capacity factor from 2006 to 2010 WRF-ARW using a REpower 5M, 5 MW turbine power curve. Isodepth contours are plotted at 30, 50 and 200 m maximum depth. The US exclusive economic zone is shown as the black dashed line.

the Mid-Atlantic to New England regions. As spring moves to summer, waters warm near Long Island and southward more rapidly than to the east and north of that region (see supporting information Figure S5 for maps of seasonal SSTs). Warmer water offshore reduces the temperature gradient between the land and the sea, hence weakening the potential for a strong sea breeze to develop. The best summer peak-time resource, and the coldest summertime SSTs (see supporting information Figure S4), can be found in the Gulf of Maine, although this is primarily deep water and would require the use of floating turbines.

A diurnal variation in the wind speed and direction is evident at buoy 44025 during April through July (see Figure 2(b)), located 38 km off Long Island, New York. In June 2010, for example, the wind has a distinct onshore flow during the peak-time (08:00–21:00 EST), with winds coming mostly out of the S or SW direction (see Figure S8). WRF-ARW 5 m height wind predictions are similar to the buoy observations (see Figure S9). The winds aloft, calculated from the closest WRF-ARW point at 90 m during June 2010, exhibit similar behavior with strong winds coming out of the W through

S directions during peak time. Such winds aloft would cause a turbine that generates rated power at 13.0 m s^{-1}, such as the REpower 5M turbine used in this study, to generate power at full capacity (5.0 MW), 19% of peak time in this example month (see Figure S10). Winds off-peak (21:00–08:00 EST) are reduced from peak-time winds during the June 2010 example, but still moderately strong. An offshore-flow from the N (see Figure S10) could likely indicate a nighttime land breeze.

If the peak-demand period changed because of large-scale implementation of load shifting technologies (e.g. electric vehicles or demand response), the peak-time OWE resource could be slightly diminished, especially in the region from Long Island, New York to Cape Cod, Massachusetts where strong sea breezes develop. Because the sea breeze resource is driven by the sun, and the current peak period is approximately matched with the solar resource, a shifting of this peak could remove the coincidence of the sea breeze and peak demand. See Dvorak *et al.*[14] for further discussion about sea-breeze-driven resources in this region.

5.3.3. Peak-demand wind energy versus depth.

Water depth is an important determinant of the economics of OWE. On the basis of the results in Table IV, only 3–4% of peak demand of the VA-to-ME region could be delivered with the use of monopile turbine foundations, which are the least costly, lowest-technology and most prevalent foundation type in the industry. However, the interannual variability of the wind resource in monopile depth class is the lowest of the three depth classes and is on the order of a fraction of a percent. This limited variability could make this resource highly valuable from a utility planning perspective. Even if our conservative assumption of only one-third of this resource being developable due to competing offshore uses is off by a factor of 2, and instead 100% more OWE is developed in this region, only <10% of peak demand in this region could be satisfied. If the threshold for development is lowered to $CF_{gross} \geq 40\%$, it is likely that up to four times more energy could be harvested in this region based on our previous analysis of the 24-hourly annual OWE resource (Table II(a and b)), although we did not calculate this explicitly. The nearshore region is arguably more susceptible to more contention over competing ocean uses (e.g. shipping lanes, beach viewsheds, military restricted ares), and only the most profitable of projects will likely be developed here.

If OWE is to satisfy more than 10% of peak demand in the VA-to-ME region, transitional turbine foundation technologies such as multi-leg tripods, quadrapods and water jackets will need to be developed at scale for the water depths from 31 to 50 m. At these depths, we find a much larger resource that, seasonally, could satisfy ≈20% of peak demand. Again, the summer season is the exception, with a significantly lower resource at these depths, especially in the Mid-Atlantic region; only 14% of the peak demand could be satisfied in the summer (Table IV and Figure 4(c)). Interannual variability is also acceptably low in this region and on the order of a few percent. Given that multi-leg turbine foundations only exist in the prototype state,[40] development at this depth range could be postponed until the foundation technologies mature and become economically viable.

Most of the VA-to-ME region peak-time demand could be satisfied with the use of floating turbine technology (51–200 m) for all seasons except summer. Interannual variability is highest at this depth range, with variability as [−7.0%, +11.2%] during the springtime. Like the shallower depths, the summertime resource is lower but also less variable. If developed, most of these turbines would be more than 100 km offshore from Virginia through Cape Cod, Massachusetts, and would not be visible from shore because of the curvature of the earth. Development in this region likely remains farther into the future, with floating turbines existing only in the prototype state[40] and the higher cost of running long-distance marine transmission cables.

By developing in all of these turbine foundation depth classes out to 200 m, it is clear that with high penetrations, most, if not all, of the peak-demand electricity in the VA-to-ME region could come from OWE ('total' row in Table IV). This is especially true for the winter, spring and fall seasons, when even the lowest year of energy production exceeds 100% of total peak energy demand. The summertime peak OWE resource is noticeably moved farther north (Figure 4(c)). This limitation during the summertime could require the large-scale development of complimentary renewable resources such as solar energy, if large reductions in GHG emissions are to be met in this region. The solar resource is inversely proportional to the wind resource, with the solar resource peaking in the summer when the wind resource is the lowest, and vice versa.

5.4. Comparison with other studies

Capps and Zender[49] (p. 4) used the Monin–Obukhov similarity theory to scale twice daily, 10 m height, $0.25 \times 0.25°$ QuikSCAT scatterometer satellite-derived winds in the greater USEC offshore area to estimate the 80 m OWE resource. The 7 years of satellite wind data, which is approximately 20×28 km resolution at 45° of latitude showed significant differences in the seasonal resource. The winter (Dec, Jan, Feb) mean wind power density (1700–3400 W m^{-2}) was found to be more than three times the summer (Jun, Jul, Aug) power (500–900 W m^{-2}). Although we did not explicitly calculate mean wind power densities as far offshore as the Capps and Zender study, we found a similar dramatic difference in

seasonal CF_{gross} during peak time. Wintertime [(Jan, Feb, Mar), Figure 4(a)] CF_{gross} numbers were $\approx$1.8 times higher than summertime CF_{gross} in some areas (Figure 4(c)).

Lu *et al.*[38] estimated the *entire* US offshore resource to be 14,000 TWh annually for bathymetry $\leq$200 m and $\leq$50 nautical miles from shore. That study placed lower restrictions on the minimum CF ($\geq$20% compared with our $\geq$40–45%), limited development to $\geq$9.2 km from shore, assumed a more dense turbine spacing ($4D \times 7D$ versus our $10D \times 10D$) and used a different wind field estimate (global, 6-hourly, $2.5 \times 2.0°$ latitude). Although these two estimates are not directly comparable, it is sufficient to say that the Lu *et al.* study illustrates the total US OWE potential if the economics of OWE become much more favorable, whereas this study assumed a much stricter requirement on the minimum CF.

Kempton *et al.*[50] found 157 and 310 GW average potential in the Mid-Atlantic Bight (Massachusetts through North Carolina), out to 50 and 100 m max water depth, respectively, by vertically extrapolating buoy measurements to the 80 m hub height (excluding the estuary resource, which was also excluded in our study). That study did not use any minimum CF cutoff but did use a comparable exclusion fraction of $\approx$30%, weighted by ocean water depth area totals (see Table 1 of Kempton *et al.*[50]). Our study found 26–57 GW average for depths $\leq$50 m and 110–157 GW average for depth $\leq$200 m (Table II), respectively, but CF_{gross} cutoffs of 45–40% included the Gulf of Maine, the region which contains the best OWE resource on the USEC, albeit deep (Figure 1). The Kempton *et al.* 50 m depth study is likely comparable with our 50 m study because much of the Gulf of Maine is deeper than 50 m. That study also found a mean CF_{gross} of 39.7% for the REpower 5M turbine (see Kempton *et al.*,[50] p. 3) for the entire study area out to 100 m depth, which means that large amounts of our study region with mean $CF_{gross} \geq$ 40% were also included in their study. Therefore, the Kempton *et al.* study found about three to six times more average power at the $\leq$50 m depth class and two to three times more average power at $\leq$100 m depth class, compared with our $\leq$200 m depth class. This difference is primarily due to the Kempton *et al.* study not including a minimum CF cutoff and not including system availability, wake and transmission losses.

The US Department of Energy's *National Renewable Energy Lab* (NREL) has created maps of mean wind speed off of the USEC (with Florida being an exception).[10] These maps are made available in GIS format.[64] To compare the mean wind speeds of the NREL maps and the ones found in this study, they created a difference map where the two maps overlapped. It was found, in general, that the NREL maps predict slightly higher mean 90 m wind speed (Figure 3(a)), with the mean and standard deviation of the difference being 0.2 and 0.3 m s^{-1}, respectively (see supporting information Figure S11 for a map of the differences). The years modeled were not given for the NREL maps, so it is possible that this could be a climatological difference from the years we modeled 2006–2010. Additionally, the cubic nature of wind power and the often non-neutral stability offshore make it difficult to derive long-term annual OWE resource from only the mean wind speed. To estimate differences in CF_{gross}, we made the standard assumption of a Rayleigh distribution of the wind speed over time and applied it to the NREL maps for the turbine used in this study with the use of an empirical method detailed in Masters[65] (p. 369) and used in Dvorak *et al.*[36] The difference in the calculated NREL CF_{gross} minus the CF_{gross} found in this study (Figure 3(c)) is as high as $\pm$13.5%, with the mean and standard deviation of the difference being 2.2% and 2.9%, respectively (see the supporting information Section S6 for methodology details and supporting information Figure S11 for a difference map).

6. CONCLUSION

This study provides maps of USEC offshore wind resources based on a high-resolution mesoscale weather model evaluated against offshore wind data. A major finding is that the strong winds off the USEC alone can theoretically power all of the annual coastal electricity demand from Florida to Maine (FL-to-ME) or about one-third of US electric power demand. With the exception of summer, all peak-time electricity demand could be satisfied in the states of Virginia through Maine (VA-to-ME) with OWE in those states' waters. This study characterized the annual mean USEC OWE resource from FL-to-ME annually and during times of peak daily and seasonal electricity demand. The interannual variability of the peak-time resource was also characterized.

Ideal locations for OWE off the USEC, irrespective of the wind resource, were identified on the basis of shallow bathymetry and low hurricane risk and accounted for the potential for conflicting ocean uses. Offshore regions were divided into depths for contemporary turbine foundation supports (1–30 m depths for monopiles and 31–50 m for multi-leg) and floating turbines (51–200 m depths). The region from VA-to-ME was found to have an abundance of shallow water, which would allow for the most cost-effective turbine foundations, monopiles, to be used *en masse* for initial development. The same region also has acceptable hurricane risk, consistent with existing offshore turbine design standards.

The annual USEC OWE resource was estimated with the use of 5 years of hourly, high-resolution (5.0 km) mesoscale model (WRF-ARW) results at the turbine hub height of 90 m for the years 2006–2010. A climatological analysis shows that these years are likely conservative estimates of the resource. Model output was shown to be skillful in the annual aggregate by validating hourly wind speed predictions against *in situ* observations from a total of 32 buoys and offshore towers spanning the USEC region. Annual, 24-hourly maps of mean wind speed, mean power density and CF based on a representative 5 MW turbine power curve integrated hourly with the use of modeled wind speeds at 90 m were created

with the 5 years of model output. System availability, wake and transmission losses were accounted for with a combined loss factor of 17.9%. Because of competing ocean uses, it was assumed that one-third of the OWE out to 30-m depth and two-thirds for 31–200 m depth could be developed.

In general, the OWE resource is best in the Gulf of Maine and Georges Banks, east of Cape Cod, Massachusetts, and generally diminishes southward. From FL-to-ME out to 200 m depth, based on the minimum turbine CF cutoffs of 45% and 40%, between 965 and 1372 TWh exists annually (110–157 GW average). Most of this capacity exists from Virginia northward, which also coincides with regions with reduced severe-hurricane risk, with annual gross CF commonly 40–50%. Between 24% and 35% of *total US* or 79–112% of total *FL-to-ME* 2009 US electricity sales could be generated with the use of USEC OWE alone if the resource was fully developed, out to 200 m depth. If only shallower waters were developed ($\leq$50 m depth), between 6–13% of US and 18–41% of USEC 2009 electricity sales could be generated with USEC OWE.

The OWE resource in the region from VA-to-ME that is coincident with peak-time electricity USEC demand was studied in detail, with interannual variability characterized. USEC electricity demand data were analyzed for 4–5 years to determine the peak electricity demand time throughout the region. The peak-time demand for the entire USEC generally occurs between 08:00 and 21:00 EST throughout the year based on a daily median–peak threshold. The OWE resource in the VA-to-ME region out to 200 m depth with annual gross $CF \geq 45\%$ could provide all of the peak-time electricity demand in the same region, even accounting for interannual variability in all seasons except for summer. Although summer months have the lowest interannual variability, only 74% of peak-time demand could be satiated. The winter and fall peak-time winds were exceptionally strong, primarily driven by powerful mid-latitude cyclones that move up the USEC. The springtime winds, although diminished from the fall and winter, remain strong, with peak-time gross CFs of 40–50% in the VA-to-ME region. Winds are lower in the summer, with peak-time gross CFs of 30–40% commonly found in shallow water regions. One peak-time spring and summertime region of interest is from Long Island, New York to Cape Cod, Massachusetts, where cold water upwelling often helps create stronger sea breezes and gross CFs stay around 40%. Additionally, if OWE is to satisfy more than 10% of peak demand in the VA-to-ME region, transitional turbine foundation technologies, such as multi-leg tripods, quadrapods and water jackets, will need to be developed at scale for the water depths from 31 to 50 m. The Gulf of Maine has the strongest summer peak-time resource, but the generally deep waters will require the development of floating turbines to tap this tremendous resource.

Although previous maps of mean wind speed have been developed over most of the USEC, this study is the first to present mean wind power density and CFs on the basis of a turbine power curve with the use of hourly wind fields from a high-resolution model, validated with offshore *in situ* data. The stringent gross-CF cutoffs used in this study of 45% and 40% limited potentially developable offshore areas to the most likely economic ones. The wind fields modeled in this study were slightly lower than previous studies with differing methodologies. These new resource maps give more insight into the amount of energy that can be harvested adjacent to the USEC by integrating a turbine curve power output over the five study years and uniquely during peak-time coastal electricity use.

The results here suggest that a vast reservoir of peak-coincident wind sits near a large population center. The extraction of such wind resource instead of the use of fossil fuels could significantly help to reduce local air pollution and global warming.

ACKNOWLEDGEMENTS

REFERENCES

1. Lu X, Tchou J, McElroy MB, Nielsen CP. The impact of production tax credits on the profitable production of electricity from wind in the U.S. *Energy Policy* 7 2011; **39**: 4207–4214.
2. Crosset KM, Culliton TJ, Wiley PC, Goodspeed TR. Population trends along the coastal United States: 1980–2008. *Technical Report*, National Oceanic and Atmospheric Administration, 2004. Available: http://oceanservice.noaa.gov/programs/mb/pdfs/coastal_pop_trends_complete.pdf. (Accessed 6 January 2009).

3. EIA. State electricity sales spreadsheet 2010. Available: http://www.eia.doe.gov/cneaf/electricity/epa/sales_state.xls. (Accessed 22 September 2011).

4. Dept of Energy. 20% wind energy by 2030: Increasing wind energy's contribution to U.S. electricity supply. *Technical Report DOE/GO-102008-2567*, 2008. Available: http://www.nrel.gov/docs/fy08osti/41869.pdf. (Accessed 01 August 2011).

5. EIA. Electric power annual data tables 2010. Available: http://www.eia.doe.gov/cneaf/electricity/epa/epa_sprdshts. html. (Accessed 22 September 2011).

6. USCB. Table 1. Annual estimates of the resident population for the United States, regions, states, and Puerto Rico: April 1, 2000 to July 1 2009, 2009. Available: http://www.census.gov/popest/states/NST-ann-est.html. (Accessed 17 February 2010).

7. Vajjhala SP, Fischbeck PS. Quantifying siting difficulty: a case study of US transmission line siting. *Energy Policy* 1 2007; **35**: 650–671.

8. PJM. 2010 state of the market report for PJM. *Technical Report*, 2010. Available: http://www.monitoringanalytics. com/reports/PJM_State_of_the_Market/2010/2010-som-pjm-volume2.pdf. (Accessed 1 September 2011).

9. Dhanju A, Kempton W. Transmission infrastructure for offshore wind power development 2007. Available: http:// www.ceoe.udel.edu/windpower/docs/OWP_Transmission_Dhan ju.pdf. (Accessed 21 July 2011).

10. Schwartz M, Heimiller D, Haymes S, Musial W. Assessment of offshore wind energy resources for the United States. *Technical Report NREL/TP-500-45889*, 2010. Available: http://www.nrel.gov/docs/fy10osti/45889.pdf. (Accessed 09 July 2010).

11. Hart EK, Stoutenburg ED, Jacobson MZ. The potential of intermittent renewables to meet electric power demand: current methods and emerging analytical techniques. *Proceedings of the IEEE* 2011; **PP**: 1–13. ID: 1.

12. Archer CL, Jacobson MZ. Supplying baseload power and reducing transmission requirements by interconnecting wind farms. *Journal of Applied Meteorology and Climatology* 2007; **46**: 1701–1717.

13. Kempton W, Pimenta F, Veron DE, Colle BA. Electric power from offshore wind via synoptic-scale interconnection. *Proceedings of the National Academy of Sciences* 2010; **107**: 7240–7245.

14. Dvorak MJ, Stoutenburg ED, Archer CL, Kempton W, Jacobson MZ. Where is the ideal location for a US East Coast offshore grid? *Geophysical Research Letters* 2012. DOI: doi:10.1029/2011GL050659, (to appear in print). in press.

15. Zhang K, Douglas BC, Leatherman SP. Twentieth-century storm activity along the U.S. East Coast. *Journal of Climate* 2000; **13**: 1748–1761.

16. Bluestein HB. *Synoptic-Dynamic Meteorology in Midlatitudes: Volume II: Observations and Theory of Weather Systems*. Oxford University Press: New York, 1993.

17. Bjerkness J, Solberg H. Life cycle of cyclones and polar front theory of atmospheric circulation. *Geofysiske Publikasjoner* 1922; **3**: 1–18.

18. Sanders F, Gyakum JR. Synoptic–dynamic climatology of the "Bomb". *Monthly Weather Review* 1980; **108**: 1589–1606.

19. Miller JE. Cyclogenesis in the Atlantic coastal region of the United States. *Journal of Meteorology* 1946; **3**: 31–44.

20. Bosart LF. England New coastal frontogenesis. *Quarterly Journal of the Royal Meteorological Society* 1975; **101**: 957–978.

21. Thomas BC, Martin JE. A synoptic climatology and composite analysis of the Alberta Clipper. *Weather and Forecasting* 2007; **22**: 315–333.

22. Comrie AC, Yarnal B. Relationships between synoptic-scale atmospheric circulation and ozone concentrations in Metropolitan Pittsburgh, Pennsylvania. *Atmospheric Environment Part B Urban Atmosphere* 9 1992; **26**: 301–312.

23. Gedzelman SD, Austin S, Cermak R, Stefano N, Partridge S, Quesenberry S, Robinson DA. Mesoscale aspects of the urban heat island around New York City. *Theoretical and Applied Climatology* 2003; **75**: 29–42.

24. Harris RI. The macrometeorological spectrum—a preliminary study. *Journal of Wind Engineering and Industrial Aerodynamics* 2008; **96**: 2294–2307.

25. Bowers L. *The effect of sea surface temperature on sea breeze dynamics along the Coast of New Jersey*, Master's Thesis, Rutgers, 2004. Available: http://archipelago.uma.pt/pdf_library/Bowers_thesis_2004_UNJ.pdf. (Accessed 02 June 2011).

26. Pullen J, Holt T, Blumberg AF, Bornstein RD. Atmospheric response to local upwelling in the vicinity of New York–New Jersey harbor. *Journal of Applied Meteorology and Climatology* 2007; **46**: 1031–1052.

27. Arritt RW. Numerical modelling of the offshore extent of sea breezes. *Quarterly Journal of the Royal Meteorological Society* 1989; **115**: 547–570.

28. Colby FP. Simulation of the New England sea breeze: the effect of grid spacing. *Weather and Forecasting* 2004; **19**: 277–285.

29. Colle BA, Novak DR. The New York Bight jet: climatology and dynamical evolution. *Monthly Weather Review* 2010; **138**: 2385–2404.

30. Frizzola JA, Fisher EL. A series of sea breeze observations in the New York City area. *Journal of Applied Meteorology* 1963; **2**: 722–739.

31. Hurrell JW, Deser C. North Atlantic climate variability: the role of the North Atlantic Oscillation. *Journal of Marine Systems* 2010; **79**: 231–244. DOI: 10.1016/j.jmarsys.2009.11.002.

32. Alexander M, Scott J. The influence of ENSO on air–sea interaction in the Atlantic. *Geophysical Research Letters* 2002; **29**: 1701, 4 pp.

33. Young IR, Zieger S, Babanin AV. Global trends in wind speed and wave height. *Science* 22 April 2011; **332**: 451–455.

34. McAdie CJ, Landsea CW, Neumann CJ, David JE, Blake ES. Tropical cyclones of the North Atlantic Ocean, 1851–2006. *Technical Report HCS6-2 1851-2006*, National Oceanic and Atmospheric Administration, 2006. Available: http://www.nhc.noaa.gov/pdf/TC_Book_Atl_1851-2006_lowres.pdf (Accessed 01 March 2011).

35. Twidell J, Gaetano G. *Offshore Wind Power*. Multi-Science Publishing Co. Ltd.: UK, Essex, 2009.

36. Dvorak MJ, Archer CL, Jacobson MZ. California offshore wind energy potential. *Renewable Energy* 2010; **35**: 1244–1254.

37. Dhanju A, Whitaker P, Kempton W. Assessing offshore wind resources: an accessible methodology. *Renewable Energy* 2008; **33**: 55–64.

38. Lu X, McElroy MB, Kiviluoma J. Global potential for wind-generated electricity. *Proceedings of the National Academy of Sciences* 2009; **106**: 10 933–10 938. DOI: 10.1073/pnas.0904101106.

39. British Oceanographic Data Centre. General Bathymetric Chart of the Oceans (GEBCO) gridded bathymetry data 2009. Available: http://www.gebco.net/data_and_products/gridded_bathymetry_data/ (Accessed 21 September 2010).

40. EWEA. Operational offshore wind farms in Europe, end 2010, 2011. Available: http://www.ewea.org/fileadmin/ ewea_documents/documents/statis tics/110214__public_offshore_wind_farms_in_Europe_2010.pdf. (Accessed 29 March 2011).

41. Henderson AR, Witcher D. Floating offshore wind energy—a review of the current status and assessment of the prospects. *Wind Engineering* 2010; **1**: 1–16.

42. Skamarock WC, Klemp JB, Dudhiha J, Gill DO, Barker DM, Duda MG, Huang X, Wang W, Powers JG. A description of the Advanced Research WRF version 3. *Technical Report NCAR/TN–475+STR*, NCAR 2008. Available: http://www.mmm.ucar.edu/wrf/users/docs/arw_v3.pdf. (Accessed 21 March 2010).

43. Dvorak MJ, Jacobson MZ. Evaluation of mesoscale modeled East Coast offshore winds using buoy data and tall towers. *American Geophysical Union Fall Meeting*, American Geophysical Union, 2010. Available: http://www.stanford.edu/~dvorak/papers/dvorak-east-coast-offshore-winds-agu-2010-final.pdf. (Accessed 16 December 2010).

44. Lange B, Larsen S, Højstrup J, Barthelmie R. Importance of thermal effects and sea surface roughness for offshore wind resource assessment. *Journal of Wind Engineering and Industrial Aerodynamics* 2004; **92**: 959–988.

45. Mesinger F, DiMego G, Kalnay E, Mitchell K, Shafran PC, Ebisuzaki W, Jović D, Woollen J, Rogers E, Berbery EH. *et al.* North American Regional Reanalysis. *Bulletin of the American Meteorological Society* 2006; **87**: 343–360.

46. Pielke Sr. RA. *Mesoscale Meteorlogical Modeling*. Academic Press: San Diego, 2002.

47. Archer CL, Jacobson MZ. Evaluation of global wind power. *Journal of Geophysical Research* 2005; **110**: D12110, 20 pp.

48. Liu WT, Tang W, Xie X. Wind power distribution over the ocean. *Geophysical Research Letters* 2008; **35**: L13808, 6 pp.

49. Capps SB, Zender CS. Global ocean wind power sensitivity to surface layer stability. *Geophysical Research Letters* 2009; **36**: L09 80, 5 pp.

50. Kempton W, Archer CL, Dhanju A, Garvine RW, Jacobson MZ. Large CO_2 reductions via offshore wind power matched to inherent storage in energy end-uses. *Geophysical Research Letters* 2007; **34**: L02817, 5 pp. DOI: 10.1029/2006GL028016.

51. Pimenta F, Kempton W, Garvine R. Combining meteorological stations and satellite data to evaluate the offshore wind power resource of Southeastern Brazil. *Renewable Energy* 11 2008; **33**: 2375–2387.

52. Barthelmie RJ, Frandsen ST, Nielsen MN, Pryor SC, Rethore PE, Jørgensen HE. Modelling and measurements of power losses and turbulence intensity in wind turbine wakes at Middelgrunden offshore wind farm. *Wind Energy* 2007; **10**: 517–528. Available: http://dx.doi.org//10.1002/we.238.

53. Arwade SR, Lackner MA, Grigoriu MD. Probabilistic models for wind turbine and wind farm performance. *Journal of Solar Energy Engineering* 2011; **133**: 041006, 9 pp. DOI: 10.1115/1.4004273. Available: http://link.aip.org/link/?SLE/133/041006/1.

54. Levitt AC, Kempton W, Smith AP, Musial W, Firestone J. Pricing offshore wind power. *Energy Policy* 2011; **39**: 6408–6421. DOI: 10.1016/j.enpol.2011.07.044.

55. Negra NB, Todorovic J, Ackermann T. Loss evaluation of HVAC and HVDC transmission solutions for large offshore wind farms. *Electric Power Systems Research* 2006; **76**: 916–927.

56. USCB. United States summary: 2000: Population and housing unit counts 2004. Available: http://www.census.gov/prod/cen2000/phc3-us-pt1.pdf. (Accessed 27 July 2011).

57. EIA. South Atlantic household electricity report 2006. Available: http://www.eia.gov/emeu/reps/enduse/er01_so-atl.html. (Accessed 8 June 2011).

58. EIA. Residential energy maps 2000: South Atlantic division 2005. Available: http://www.eia.gov/emeu/reps/recmap/rec_so-atl.html. (Accessed 8 June 2011).

59. EIA. Regional energy profile: Middle Atlantic data abstract 2005. Available: http://www.eia.gov/emeu/reps/abstracts/mid_atl.html. (Accessed 8 June 2011).

60. EIA. Regional energy profile: New England data abstract 2005. Available: http://www.eia.gov/emeu/reps/abstracts/new_eng.html. (Accessed 8 June 2011).

61. EIA. Regional energy profile: Northeast data abstract 2003. Available: http://www.eia.gov/emeu/reps/abstracts/northeast.html. (Accessed 8 June 2011).

62. Cape Wind Associates LLC. Comparison of cape wind scientific data tower wind speed data with ISO New England list of top ten electric demand days. *Technical Report*, 2007. Available: http://www.capewind.org/downloads/CWReport.pdf. (Accessed 17 January 2011).

63. Casey KS, Kearns EJ, Halliwell V, Evans R. Seasonal sea surface temperature averages, 1985–2001, 2004. Available: http://nationalatlas.gov/mld/sstalli.html. (Accessed 26 September 2011).

64. NREL. Atlantic Coast 90m windspeed offshore wind high resolution, GIS Shp file, 2010. Available: http://www.nrel.gov/gis/data_wind.html. (Accessed 05 August 2011).

65. Masters GM. *Renewable and Efficient Electric Power Systems*. John Wiley & Sons: NJ, Hoboken, 2004.